

Prediction of Static Liquefaction Landslides

Abouzar Sadrekarimi

Department of Civil & Environmental Engineering, Western University, London, Ontario, Canada



ABSTRACT

Static liquefaction failure of sloping grounds has resulted in significant damages to built structures and even loss of lives. The principal aim of this research is to relate static liquefaction behavior of cohesionless soils to a measurable threshold from the field. Based on a very large number (893) of undrained laboratory shear tests on cohesionless soils collected from the past literature, a threshold triggering excess pore water pressure is introduced in this study above which static liquefaction failure occurs. The effect of variations in the direction and relative magnitudes of principal stresses associated with different modes of shear and ground slopes on static liquefaction failure of cohesionless soils is characterized by empirical relationships of the triggering excess pore water pressure ratio with these variables. The triggering pore pressure ratio can be employed as a more precise criterion for detecting liquefaction triggering and landslide warning in instrumented slopes of saturated cohesionless soils.

RÉSUMÉ

L'échec de la liquéfaction statique des sols en pente a provoqué des dommages importants aux structures construites et même des pertes de vies humaines. Le but principal de cette recherche est de relier le comportement statique de liquéfaction de sols sans cohésion à un seuil mesurable du terrain. Sur la base d'un très grand nombre (893) d'essais de cisaillement en laboratoire non drainés sur des sols sans cohésion, relevés dans la littérature antérieure, un seuil déclenchant une pression interstitielle en excès est introduit dans cette étude, au-dessus duquel se produit une défaillance de liquéfaction statique. L'effet des variations dans la direction et les amplitudes relatives des principales contraintes associées à différents modes de cisaillement et de pentes du sol sur l'échec de la liquéfaction statique de sols sans cohésion est caractérisé par des relations empiriques du rapport de déclenchement de la pression de l'eau dans les pores excédentaire avec ces variables. Le rapport de pression interstitielle de déclenchement peut être utilisé comme critère plus précis pour détecter le déclenchement de la liquéfaction et l'avertissement de glissement de terrain sur les pentes instrumentées de sols saturés et sans cohésion.

1 INTRODUCTION

Most landslides in steep slopes are triggered by increasing of excess pore water pressure (generated by a seismic event, heavy rainfall, rapid snowmelt, tidal fluctuations, water waves, pile driving, or rapid changes in water level), leading to an undrained static liquefaction failure and strain-softening. During this phenomenon, rise in pore water pressure reduces soil's effective stress and thus shear resistance, and eventually leads to a slope failure. This can develop into a catastrophic flow slide failure if the post-liquefaction strength of the soil drops below the static driving shear stress beneath the slope. The sudden nature and the large shear displacements attained rapidly following flow liquefaction events have made static liquefaction one of the most catastrophic mechanisms in the failure of natural slopes, man-made dams, and mine tailings embankments.

Despite considerable advances in understanding landslide mechanics and the employment of landslide monitoring systems, these phenomena continue to cause significant damages throughout the world. For example, the deadliest landslide disaster in the United State's history occurred on the 22th of March 2014 in Oso, Washington (USA) after three weeks of intense rainfall. The Oso landslide mass obliterated more than 50 homes, claimed 43 lives, injured 10 people, and buried portions of a major state highway resulting to an estimated capital loss of at

least \$50 million. The failure occurred in a loose sandy colluvial material susceptible to static liquefaction (Keaton, et al., 2014). Even more recently, the Fundão iron mine tailings dam (Brazil) failed due to static liquefaction on November 5th, 2015. Static liquefaction failure resulted from a clogged drainage and the subsequent increase in pore water pressure (Morgenstern et al., 2016). Although some studies have proposed empirical rainfall thresholds, such thresholds can be often misleading and erratic without proper consideration of the mechanisms of failure and the role of pore water pressure.

Previous experimental studies of flow slide failures indicate that the initiation of liquefaction flow failure is essentially associated with the build-up of excess pore water pressure (u_e) and the corresponding reduction in effective stress and soil resistance (Anderson and Sitar, 1995; Eckersley, 1990; Take, et al., 2013). With a sufficient increase in u_e , a saturated sandy slope can undergo undrained strain-softening and static liquefaction. Accordingly, an analysis of the threshold u_e required for static liquefaction failure can be effectively used to predict the occurrence of a flow failure. However, just how much u_e is required to produce a flow slide has not yet been resolved. This study attempts to relate static liquefaction behavior to an experimentally-verifiable threshold of pore water pressure above which liquefaction occurs. A practical framework for predicting the onset of static liquefaction is presented based on a minimum triggering u_e required to

induce undrained strain-softening in a saturated cohesionless soil.

2 THRESHOLD EXCESS PORE PRESSURE RATIO

Figure 1 presents undrained triaxial compression shear tests on Illinois River and Toyoura sand specimens in terms of consolidation relative density (D_{rc}) and excess pore pressure ratio (r_u). Several studies (Ishihara, 2008; Vaid and Chern, 1983) have found that the major principal stress at the time of consolidation (σ'_{1c}) largely controls liquefaction and shearing behavior of cohesionless soils. Accordingly, r_u is defined here as the shear-induced excess pore water pressure (u_e) normalized by σ'_{1c} . Static liquefaction and undrained strength reduction is triggered when the applied monotonic shear load exceeds soil's peak undrained strength, $s_u(\text{yield})$. Strain-softening subsequently follows the initiation of liquefaction until a reduced post-liquefaction undrained strength, $s_u(\text{liq})$ is mobilized.

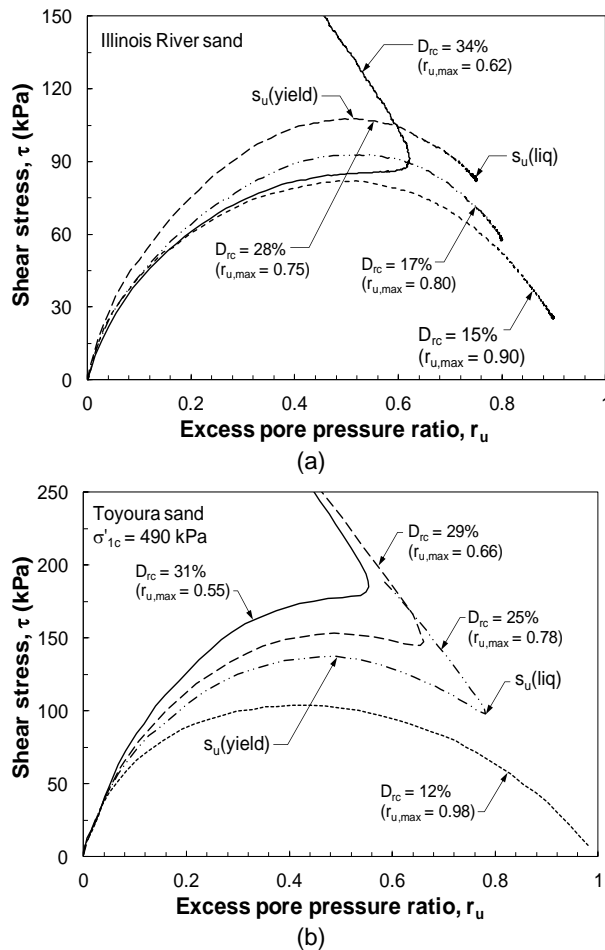


Figure 1. Undrained shearing behavior and the generation of $r_{u,max}$ in triaxial compression shear tests on (a) Illinois River and (b) Toyoura sand specimens.

According to Figure 1, with increasing D_{rc} the amount of strength reduction from $s_u(\text{yield})$ to $s_u(\text{liq})$ and r_u decrease until at $D_{rc} = 34\%$ and 31% neither of the sands display strain-softening and liquefaction behavior. The maximum r_u ($r_{u,max}$) developed in specimens which exhibit even the slightest strain-softening behavior are all greater than 0.64 for both Illinois River and Toyoura sand specimens. Whereas, those at respectively $D_{rc} = 34\%$ and 31% for Illinois River and Toyoura sands undergo strain-hardening behavior with $r_{u,max} < 0.64$. These suggest that the occurrence of static liquefaction in a saturated cohesionless soil is closely related to $r_{u,max}$.

Although $r_{u,max} = 0.64$ is inferred from Figure 1, field liquefaction behavior and pore water pressure generation in a soil beneath a sloping ground can be more complicated than an isotropically-consolidated specimen. Figure 2 illustrates a hypothetical failure plane beneath a sloping ground. Different modes of shearing, ranging from compression at the crest of the slope, to simple shear, and extension at the toe can exist on a failure plane. As illustrated in Figure 2, a transition in mode of shearing occurs as the angle of the failure plane with the horizontal varies and the associated principal stress (σ'_1 , σ'_3) directions rotate (Yoshimine, et al., 1999). Different modes of shearing are approximately assigned along the failure plane in Figure 2 based on the counter-clockwise angle of the failure plane to the horizontal (θ), with $\theta > 15^\circ$, $-15^\circ \leq \theta \leq 15^\circ$, and $\theta < -15^\circ$ attributed as compression, simple shearing, and extension modes of shear, respectively. The relative magnitudes of the initial (consolidation) principal stresses (σ'_{1c} , and σ'_{3c}) under a sloping ground also change, which produces different principal stress anisotropy characterized by the principal stress ratio, $K_c = \sigma'_{3c}/\sigma'_{1c}$.

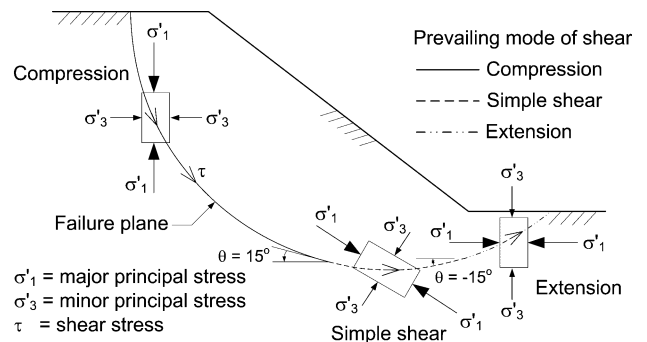


Figure 2. Illustrative variation of principal stress directions and mode of shearing along a failure plane beneath a slope.

As demonstrated in Figure 3, $r_{u,max}$ developed in a cohesionless soil is largely affected by differences in triaxial compression (TxC), direct simple shear (SS), and triaxial extension (TxE) modes of shear as well as K_c and D_{rc} . Accordingly, for a precise prediction of r_u required to trigger static liquefaction ($r_{u,tr}$) it is necessary to account for the variation in principal stress directions associated with different modes of shearing and their relative magnitudes (K_c) beneath a sloping ground. Based on a large database

of laboratory shear tests collected from past studies, this study explores a threshold r_u ($r_{u,tr}$) beyond which static liquefaction could occur in a cohesionless soil. The effects of K_c and differences in mode shearing on $r_{u,tr}$ are also studied.

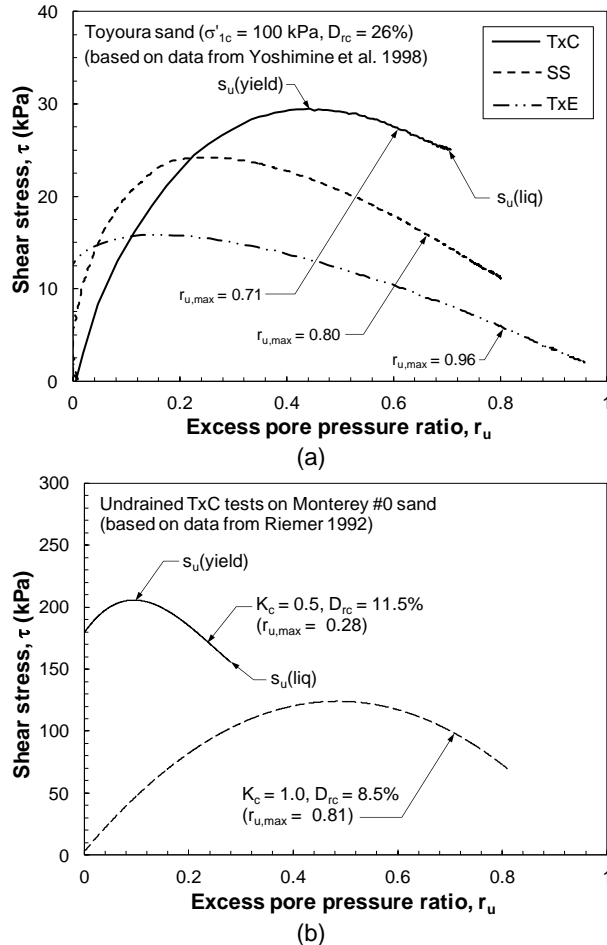


Figure 3. Effects of (a) shearing mode (TxC: triaxial compression, SS: direct simple shear, TxE: triaxial extension), and (b) principal stress anisotropy (K_c) on undrained shearing behaviors of Toyoura and Monterey sands.

3 DATABASE OF LABORATORY SHEAR TESTS

A large database of 873 triaxial compression shear, TxC (Castro, 1969; Chen, 1984; Chu, 1995; Dawson, et al., 1998; de Gregorio, 1990; Dennis, 1988; Di Prisco, et al., 1995; Doanh, et al., 1997; Durham and Townsend, 1973; Finge, et al., 2006; Fourie and Tshabalala, 2005; Gajo and Piffer, 1999; Gassman, 1994; Hightner and Tobin, 1980; Hightner and Vallee, 1980; Hird and Hassona, 1990; Hyodo, et al., 1994; Jefferies and Been, 2006; Kato, et al., 2001; Konrad, 1993; Konrad and Pouliot, 1997; Kramer and Seed, 1988; Lavigne, 1988; Lee, 1965; Leong and Chu, 2002; Murthy, et al., 2007; Omar, 2013; Riemer, 1992; Sadrekarimi, 2009; Sasitharan, 1994; Sasitharan, et al.,

1994; Skirrow, 1996; Sladen, et al., 1985; Sladen and Handford, 1987; Stiber, 1992; Takeshita, et al., 1995; Tsomokos and Georgiannou, 2010; Vaid, et al., 2001; Verdugo, 1992; Wanatowski and Chu, 2007; Wang, 2005; Wride and Robertson, 1997a; Wride and Robertson, 1997b; Yoshimine, 1996; Zhang, 1997), torsional simple shear, TSS (Alarcon-Guzman, et al., 1988; Keyhani and Haeri, 2013; Nakata, et al., 1998; Sivathayalan and Vaid, 2002; Wride and Robertson, 1997a; Yoshimine and Ishihara, 1998; Yoshimine, et al., 1999), and triaxial extension shear, TxE (Been, et al., 1991; Chung, 1985; Doanh, et al., 1997; Gajo and Piffer, 1999; Hyodo, et al., 1994; Lade, et al., 2006; Riemer, 1992; Shahsavari, 2012; Vaid, et al., 2001; Vaid and Thomas, 1995; Yoshimine, et al., 1998; Yoshimine, et al., 2001; Yoshimine, et al., 1999) tests on cohesionless soils are collected in this study which cover a very wide range of non-plastic silt contents, SC (0 to 60%), consolidation void ratios, e_c (0.261 to 1.287), major consolidation principal stresses, σ'_{1c} (29 to 60,000 kPa), specimen preparation techniques (AP: air pluviation; WP: water pluviation; MT: moist tamping), and consolidation principal stress ratios, K_c (0.33 to 1.0). The wide range of K_c (0.33 to 1.0) allows the modeling of different sloping ground initial conditions. Principal stress directions continuously rotate in TSS tests or undergo an abrupt 90° rotation in TxE shearing of anisotropically consolidated specimens, while the principal stress directions remain the same in TxC tests. Note that shear stress is applied in TSS tests by torsion, while TxC and TxE samples undergo shearing on the failure plane as a result of a deviator stress.

As shown in Figure 1, $s_u(\text{yield})$ and $s_u(\text{liq})$ respectively describe the liquefaction triggering condition and the subsequent behavior after liquefaction occurs. Following the triggering of liquefaction, the mobilized undrained strength reduces from $s_u(\text{yield})$ to $s_u(\text{liq})$. The normalized difference between $s_u(\text{yield})$ and $s_u(\text{liq})$ is used here to quantify the degree of strain-softening and determine the occurrence of static liquefaction. This is often defined by the undrained brittleness index, I_B as below (Bishop, 1971):

$$I_B = \frac{s_u(\text{yield}) - s_u(\text{liq})}{s_u(\text{yield})} \quad [1]$$

I_B ranges from 0 to 1, where $I_B = 1$ indicates a very brittle soil behavior associated with an extremely low $s_u(\text{liq})$, while $I_B = 0$ occurs in non-brittle or strain-hardening soils where no strength reduction occurs during undrained shear.

In the following, the liquefaction behavior of cohesionless soils is characterized in terms of I_B and $r_{u,max}$ for the 873 laboratory shear tests collected in this study. Note that $s_u(\text{yield})$ includes the initial shear stress (τ_c) resulting from anisotropic consolidation, as well as the additional shear stress applied to cause strain-softening and liquefaction. The post-liquefaction undrained strength, $s_u(\text{liq})$ is chosen at the end of the tests where a critical state of constant effective stress and shear stress is attained following strain-softening behavior. Whereas, for specimens exhibiting a limited liquefaction the minimum undrained strength prior to strain-hardening is more relevant to flow

failures and stability analysis and this is adopted here as $s_u(\text{liq})$.

4 RESULTS AND DISCUSSION

Figure 4 presents I_B versus $r_{u,\max}$ for each mode of shear based on the large database of laboratory shear tests. While I_B and the amount of strain-softening increase with increasing $r_{u,\max}$ for all modes of shearing, these plots show greater $r_{u,\max}$ in compression and simple shearing modes than when a soil is subject to an extension mode of shear. The plots of Figure 4 further indicate that increasing anisotropic consolidation (decreasing K_c) promotes strain softening and increases I_B .

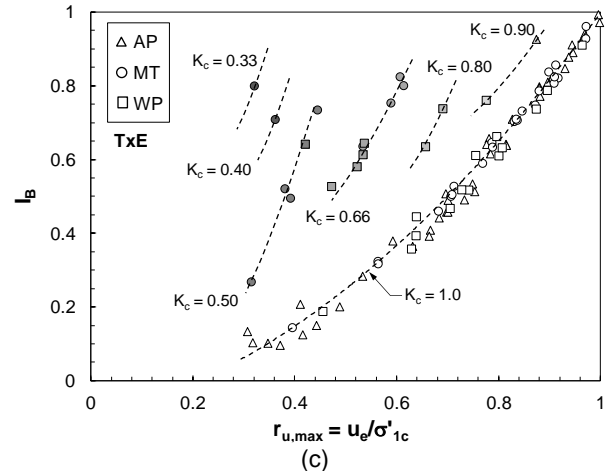
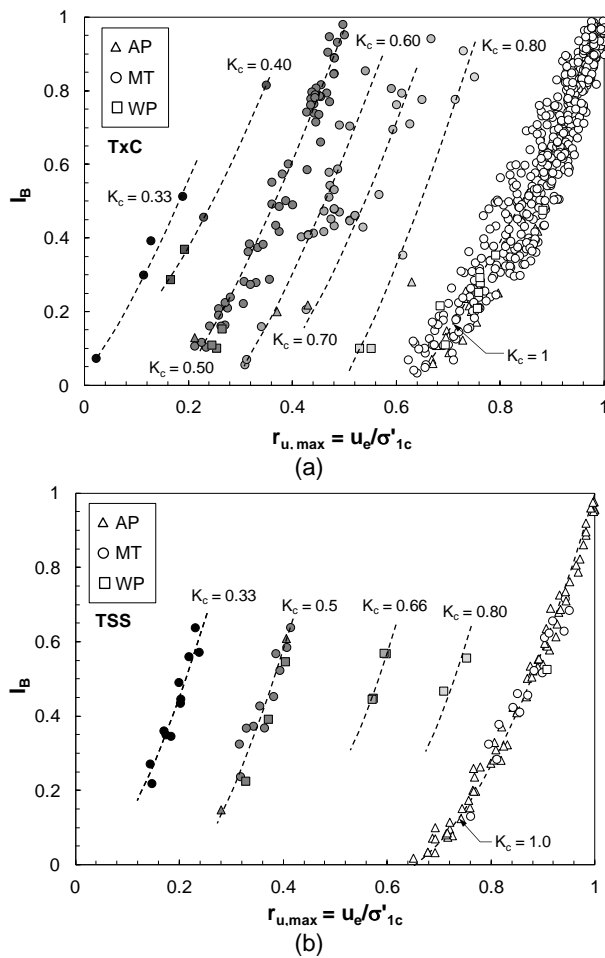


Figure 4. Undrained brittleness (I_B) and maximum excess pore water pressure ratio ($r_{u,\max}$) data for (a) TxC, (b) TSS, and (c) TxE shear tests.

An interesting feature of Figure 4 is that the $r_{u,\max} - I_B$ data fall on a distinct trendline for each K_c , inferring that $r_{u,\max}$ is primarily affected by K_c and the mode of shearing for saturated granular soils. The small scatter at a given K_c for each mode of shear possibly emerges from differences in SC, specimen preparation method (i.e. soil fabric), e_c and σ'_{1c} , besides inaccuracies in laboratory shear testing of loose sands at large shear strains (e.g., membrane resistance, bedding errors, boundary effects, non-uniform stress distribution associated with specimen bulging in TxC and necking in TxE). It follows that a state of $r_{u,\max} = 1.0$ ($\sigma_3 = 0$) is only possible for isotropically consolidated soils ($K_c = 1$), while for anisotropically consolidated cohesionless soils ($K_c < 1$) severe strain-softening and $I_B \approx 1$ could ensue at $r_{u,\max} < 1.0$.

For each mode of shearing in Figure 4, the average $r_{u,\max} - I_B$ trendline for each K_c resembles that of $K_c = 1$ which is translated both horizontally (decreasing $r_{u,\max}$) and vertically (increasing I_B) in proportion to its K_c value. Accordingly, modified I_B^* and $r_{u,\max}^*$ parameters are used to shift these data onto the $K_c = 1$ trendline in Figure 5. Figure 5 further presents specific correlations between I_B^* and $r_{u,\max}^*$ for each mode of shear which include the effects of K_c . Despite the wide ranges of testing parameters (e_c , SC, σ'_{1c} , K_c , specimen preparation methods), correlations shown in Figure 5 display a relatively narrow range of variations and the average relationships exhibit high coefficients of correlation (R^2) indicating their accuracy.

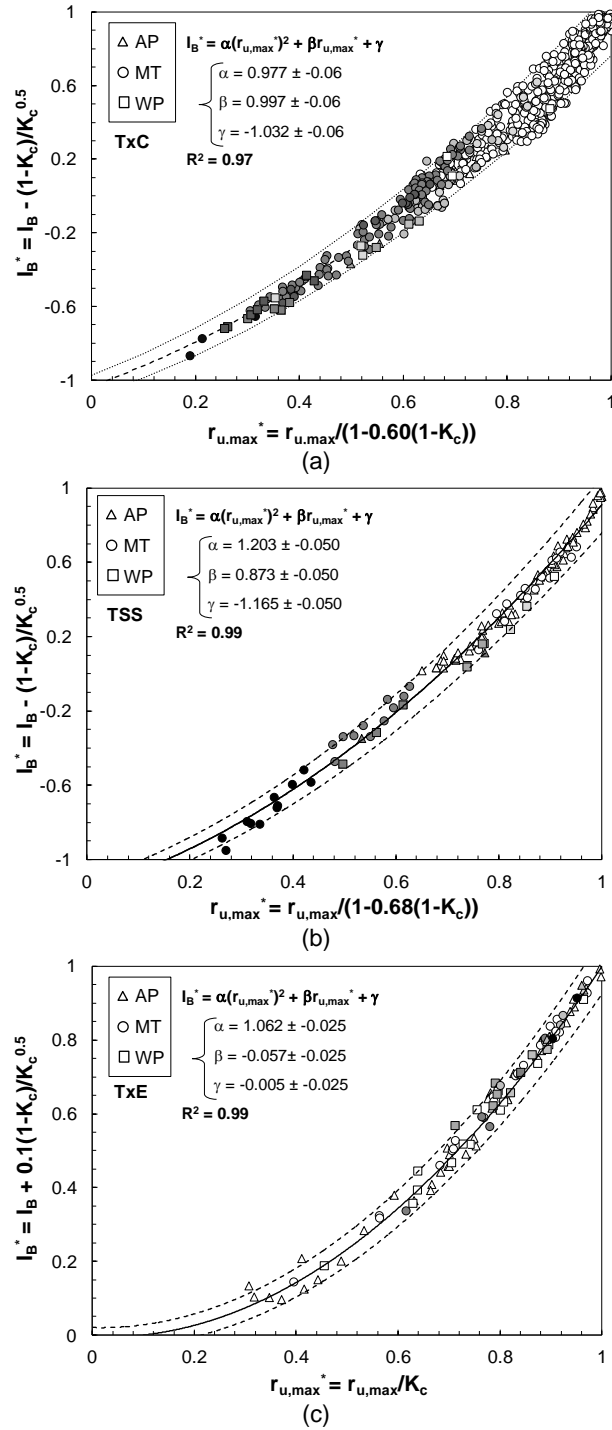


Figure 5. Unified relationships based on modified I_B^* and r_u^* data for (a) TxC, (b) TSS, and (c) TxE shear tests.

5 TRIGGERING OF STATIC LIQUEFACTION

Static liquefaction could trigger when a soil is no longer able to sustain the applied shear stress and hence undergoes strain-softening ($I_B \geq 0$). Therefore, $I_B = 0$ would represent the minimum condition to instigate static

liquefaction behavior as well as the threshold r_u ($r_{u,tr}$) above which a saturated cohesionless soil will liquefy ($I_B > 0$). The relationships shown in Figure 5 can thus be used to estimate the ranges of $r_{u,tr}$ corresponding to the initiation of static liquefaction ($I_B \geq 0$) for each shearing mode.

At any given K_c , a range of I_B^* is obtained from its relationship with I_B as shown in the abscissa of Figure 5 for each mode of shearing and sweeping I_B from 0 to 1.0. Based on the fitted correlation between I_B^* and $r_{u,tr}^*$ for each shearing mode, $r_{u,tr}$ is then calculated from $r_{u,tr}^*$ using the corresponding equation between $r_{u,tr}$ and $r_{u,tr}^*$ shown in the ordinates of Figure 5. The variation of $r_{u,tr}$ with K_c is subsequently demonstrated in Figure 6 for each mode of shearing. According to this figure, $r_{u,tr}$ increases with increasing K_c for compression and simple shearing modes. In other words, the potential for static liquefaction failure would increase (i.e. failure occurs earlier at a lower $r_{u,tr}$) with increasing ground slope. Griffiths et al. (2011) and Eichenberger et al. (2013) report similar trends respectively for saturated cohesive soils and volcanic ash in finite element simulations. In extension however, since anisotropic consolidation pre-shearing (K_c) and undrained extensional shearing occur in different directions, shear stress reversal occurs on the failure plane in TxE tests, and thus $r_{u,tr}$ exhibits a brief increase with decreasing K_c followed by a more-or-less constant $r_{u,tr} = 0.136$. Accordingly, in order to obtain more accurate estimates of $r_{u,tr}$ for triggering analysis it is imperative to consider the appropriate K_c corresponding to the operating mode of shear and the in-situ stress condition. Note that although $r_{u,tr}$ seems to be independent of D_{rc} , this can be considered by measuring the in-situ r_u as D_{rc} affects a soil's ability to develop excess pore pressure and attain $r_{u,tr}$ for instigating liquefaction.

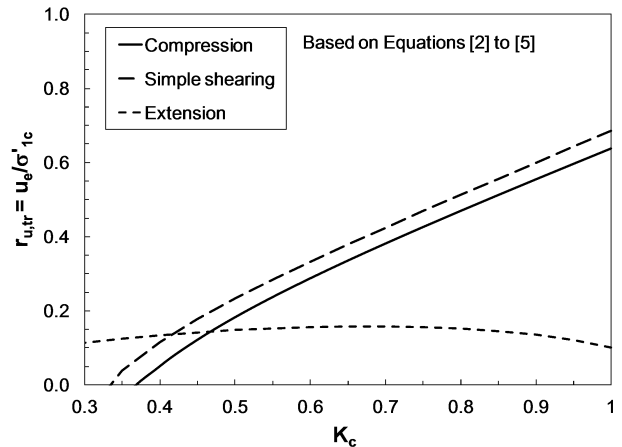


Figure 6. Effect of anisotropic consolidation (K_c) on $r_{u,tr}$

6 APPLICATION FOR STATIC LIQUEFACTION PREDICTION

It is proposed that $r_{u,tr}$ can provide a refined criterion for examining field stress paths and determining the proximity of an in-situ stress state to instability. The proposed method can be employed as a pragmatic triggering

criterion in landslide warning and in-situ monitoring systems for enhanced prediction of flow slide failures resulting from static liquefaction. This would require warning pore water pressure thresholds to be set with respect to $r_{u,tr}$ for the corresponding mode of shear and stress anisotropy (K_c). A drained limit equilibrium analysis of the pre-failure slope geometry should be first performed to identify the probable critical sliding surface (with the lowest factor of safety) and establish the pre-failure (consolidation) shear (τ_c) and normal (σ'_{nc}) stresses along the sliding surface. The magnitude of K_c along a potential failure plane can be determined from the following equation (Ishihara, 2008):

$$K_c = \frac{\sigma'_{3c}}{\sigma'_{1c}} = \frac{\sigma'_{nc} - \tau_c / \cos \theta + \tau_c \tan \theta}{\sigma'_{nc} + \tau_c / \cos \theta + \tau_c \tan \theta} \quad [6]$$

An infinite slope is a special case of Equation [6] in which the sliding plane is parallel to the ground slope ($\alpha = \theta$), and thus $K_c = (1 - \sin \alpha)/(1 + \sin \alpha)$ beneath an infinite slope of an angle α .

Similar to Figure 2, approximate modes of shear can be assigned based on the inclination of the failure plane from the horizontal (θ), with $\theta > 15^\circ$, $-15^\circ \leq \theta \leq 15^\circ$, and $\theta < -15^\circ$ corresponding to compression, simple shearing, and extension modes of shear, respectively. Relationships shown in Figure 5 can then be employed to calculate $r_{u,tr}$ on the failure plane and predict liquefaction-induced landslides. The critical sliding surface (determined from a limit equilibrium analysis) can be used as a preliminary guideline for the installation of piezometers for measuring u_e along the probable failure surface. An ideal field monitoring system would be automated with sufficient measurement points to examine the pattern of pore water pressure generation and identify the most critical pore pressure regime on a real-time basis. The strength of the proposed method is that the in-situ r_u is directly measured by piezometers, and there is no need for expensive soil sampling or the determination of in-situ density of cohesionless soils. The key contribution of this method is that the fundamental effects of mode of shearing and K_c are considered in predicting static liquefaction and $r_{u,tr}$.

Note that the proposed method is only applicable when a slope has become fully saturated. In an unsaturated soil, suction among soil particles imparts additional confining stress which could create steep slopes ($\alpha \geq 30^\circ$). If saturated (e.g., by a rainfall, tidal fluctuation, snowmelt), the decrease of soil suction and the increase of soil unit weight (as water infiltrates soil) can produce a rapid accumulation of shear strain and positive u_e . Due to steep slopes (high K_c), $r_{u,tr}$ required to instigate static liquefaction failure could be quickly attained.

7 CONCLUSIONS

This study suggests a certain threshold of pore water pressure ratio ($r_{u,tr}$) required to trigger static liquefaction and produce undrained strain-softening behavior. The

threshold excess pore water pressure ratio defines a boundary between liquefaction and non-liquefaction behaviors based on a large number of high-quality laboratory shear test results. The laboratory test results indicate that excess pore pressure equal to the total overburden pressure (i.e., $r_u = 100\%$) is not necessarily required for static liquefaction triggering, and failure could occur at a much lower $r_{u,tr}$. It is further observed that $r_{u,tr}$ mobilized in compression and simple shearing modes decrease with increasing initial stress anisotropy (decreasing K_c). Whereas for extension shearing, K_c has a relatively reduced effect on $r_{u,tr}$.

Based on the premise that $r_{u,tr}$ is developed just before the occurrence of static liquefaction, an empirical approach is developed in this study for estimating $r_{u,tr}$. The concept of triggering pore pressure recognizes that pore pressure is central to liquefaction and flow failures, and it is based on the principles that stress anisotropy and mode of shearing determine liquefaction potential and $r_{u,tr}$ produced in a cohesionless soil subject to a monotonic shear load. The results of this study provide the possibility to develop more precise early warning systems based on the measurement of pore water pressure required for triggering liquefaction-induced landslides. Soil characteristics such as relative density, silt content, or fabric are indirectly considered by measuring and monitoring of the in-situ r_u , while slope geometry is accounted for through K_c .

8 REFERENCES

- Alarcon-Guzman, A., Leonards, G. A., and Chameau, J. L. (1988). "Undrained monotonic and cyclic strength of sands." *Journal of Geotechnical Engineering Division*, ASCE, 114(10): 1089 - 1109.
- Anderson, S. A., and Sitar, N. (1995). "Analysis of rainfall-induced debris flows." *Journal of Geotechnical Engineering*, ASCE, 121(7): 544 - 552.
- Been, K., Jefferies, M. G., and Hachey, J. (1991). "The critical state of sands." *Geotechnique*, 41(3): 365 - 381.
- Bishop, A. W. (1971). "Shear strength parameters for undisturbed and remoulded soil specimens." *Proc., Roscoe Memorial Symposium*, 3-58.
- Chen, H. W. (1984). "Stress-strain and volume change characteristics of tailings materials." PhD, University of Arizona, Tucson, Arizona.
- Chu, J. (1995). "An experimental examination of the critical state and other similar concepts for granular soils." *Canadian Geotechnical Journal*, 32(6): 1065 - 1075.
- Chung, E. K. F. (1985). "Effects of stress path and prestrain history on the undrained monotonic and cyclic loading behaviour of saturated sand." MEng, University of British Columbia, Vancouver.
- Davis, A. P., Poulos, S. J., and Castro, G. (1988). "Strengths backfigured from liquefaction case histories." *Second International Conference on Case Histories in Geotechnical Engineering*, St. Louis, MO, pp. 1693-1701.
- Dawson, R. F., Morgenstern, N. R., and Stokes, A. W. (1998). "Liquefaction flowslides in Rocky Mountain coal mine waste dumps." *Canadian Geotechnical Journal*, 35(2): 328-343.

- de Gregorio, V. B. (1990). "Loading systems, sample preparation, and liquefaction." *Journal of Geotechnical Engineering Division*, ASCE, 116(5): 805 - 821.
- Dennis, N. D. (1988). "Influence of specimen preparation techniques and testing procedures on undrained steady state shear strength." *Advanced Triaxial Testing of Soil and Rock*, ASTM STP 977, R. T. Donaghe, R. C. Chaney, and M. L. Silver, eds., American Society for Testing and Materials, Philadelphia, pp. 642 - 654.
- Di Prisco, C., Mantiotti, R., and Nova, R. (1995). "Theoretical investigation of the undrained stability of shallow submerged slopes." *Geotechnique*, 45(3): 479 - 496.
- Doanh, T., Ibraim, E., and Mantiotti, R. (1997). "Undrained instability of very loose Hostun sand in triaxial compression and extension. Part 1: experimental observations." *Mechanics of Cohesive-Frictional Materials*, Vol. 2, pp. 47 - 70.
- Durham, G. N., and Townsend, F. C. (1973). "Effect of relative density on the liquefaction susceptibility of a fine sand under controlled-stress loading." *Evaluation of Relative Density and its Role in Geotechnical Projects Involving Cohesionless Soils*, ASTM STP 523, American Society for Testing and Materials, pp. 319 - 331.
- Eckersley, J. (1990). "Instrumented laboratory flowslides." *Geotechnique*, 40(3): 489 - 502.
- Finge, Z., Doanh, T., and Dubujet, P. (2006). "Undrained anisotropy of Hostun RF loose sand: new experimental investigations." *Canadian Geotechnical Journal*, 43(11): 1195 - 1212.
- Gajo, A., and Piffer, L. (1999). "The effects of preloading history on the undrained behaviour of saturated loose sand." *Soils and Foundations*, 39(6): 43 - 54.
- Gassman, S. L. (1994). "Undrained steady state shear strength and instabilities of fine sands." PhD, Northwestern University, Evanston, Illinois.
- Highter, W. H., and Tobin, R. F. (1980). "Flow slides and the undrained brittleness index of some mine tailings." *Engineering Geology*, 16(1-2): 71 - 82.
- Highter, W. H., and Vallee, R. P. (1980). "The liquefaction of different mine tailings under stress controlled loading." *Engineering Geology*, 16(1-2): 147 - 150.
- Hird, C. C., and Hassona, F. A. K. (1990). "Some factors affecting the liquefaction and flow of saturated sands in laboratory tests." *Engineering Geology*, 28(1-2): 149 - 170.
- Hyodo, M., Tanimizu, H., Yasufuku, N., and Murata, H. (1994). "Undrained cyclic and monotonic triaxial behavior of saturated loose sand." *Soils and Foundations*, 34(1): 19 - 32.
- Ishihara, K. (1993). "Liquefaction and flow failure during earthquakes." *Geotechnique*, 43(3): 351 - 415.
- Ishihara, K. (2008). "Flow slides of underwater sand deposits in Jamuna River bed." *Proc., Geotechnical Engineering for Disaster Mitigation and Rehabilitation: Proceedings of the 2nd International Conference GEDMAR08*, Springer Berlin Heidelberg, pp. 3 - 34.
- Iverson, R. M., Reid, M. E., and LaHusen, R. G. (1997). "Debris-flow mobilization from landslides." *Annual Review of Earth and Planetary Sciences*, 25: 85 - 138.
- Jefferies, M. G., and Been, K. (2006). *Soil liquefaction - a critical state approach*, Taylor & Francis, New York.
- Kato, S., Ishihara, K., and Towhata, I. (2001). "Undrained shear characteristics of saturated sand under anisotropic consolidation." *Soils and Foundations*, 41(1): 1-11.
- Keaton, J. R., Wartman, J., Anderson, S. A., Benoît, J., de La Chapelle, J., Gilbert, R., and Montgomery, D. R. (2014). "The 22 March 2014 Oso Landslide, Snohomish County, Washington." *Turning Disaster into Knowledge, Geotechnical Extreme Events Reconnaissance*, 172 p.
- Keyhani, R., and Haeri, S. M. (2013). "Evaluation of the effect of anisotropic consolidation and principle stress rotation on undrained behavior of silty sands." *Scientia Iranica A*, 20(6): 1637 - 1653.
- Konrad, J. M. (1993). "Undrained response of loosely compacted sands during monotonic and cyclic compression tests." *Geotechnique*, 43(1): 69 - 89.
- Konrad, J. M., and Pouliot, N. (1997). "Ultimate state of reconstituted and intact samples of deltaic sand." *Canadian Geotechnical Journal*, 34(5): 737-748.
- Kramer, S. L., and Seed, B. H. (1988). "Initiation of static liquefaction under static loading conditions." *Journal of Geotechnical Engineering*, ASCE, 114(4): 412 - 430.
- Lade, P. V., Yamamuro, J. A., and Bopp, P. A. (2006). "Drained and undrained strengths of sand in axisymmetric tests at high pressures." *Proc., Second Japan-U.S. Workshop on Testing, Modeling, and Simulation in Geomechanics*, American Society of Civil Engineers (ASCE), pp. 87 - 102.
- Lavigne, T. A. (1988). "The effects of anisotropic consolidation on the liquefaction potential of mine tailings." Master of Science, Clarkson University, Potsdam, New York.
- Lee, K., L. (1965). "Triaxial compressive strength of saturated sand under seismic loading conditions." PhD, University of California, Berkeley.
- Leong, W. K., and Chu, J. (2002). "Effect of undrained creep on instability behaviour of loose sand." *Canadian Geotechnical Journal*, 39(6): 1399-1405.
- Lindenberg, J., and Koning, H. L. (1981). "Critical density of sand." *Geotechnique*, 31(2): 231 - 245.
- McRoberts, E. C., and Sladen, J. A. (1992). "Observations on static and cyclic sand-liquefaction methodologies." *Canadian Geotechnical Journal*, 29(4): 650 - 665.
- Morgenstern, N. R., Vick, S. G., Viotti, C. B., and Watts, B. D. (2016). "Report in the immediate causes of the failure of the Fundão Dam." Fundão Tailings Dam Review Panel.
- Murthy, T. G., Loukidis, D., Carraro, J. A. H., Prezzi, M., and Salgado, R. (2007). "Undrained monotonic response of clean and silty sands." *Geotechnique*, 57(3): 273 - 288.
- Nakata, Y., Hyodo, M., Murata, H., and Yasufuku, N. (1998). "Flow Deformation of Sands Subjected to Principal Stress Rotation." *Soils and Foundations*, 38(2): 115-128.
- Okura, Y., Kitahara, H., Ochiai, H., Sammori, T., and Kawanami, A. (2002). "Landslide fluidization process by flume experiments." *Engineering Geology*, 66(1-2): 65 - 78.

- Omar, T. (2013). "Specimen size effect on shear behavior of loose sand in triaxial testing." MSc, Western University, London.
- Riemer, M. F. (1992). "The effects of testing conditions on the constitutive behavior of loose, saturated sand under monotonic loading." PhD, University of California, Berkeley, California.
- Riemer, M. F., and Seed, R. B. (1997). "Factors affecting apparent position of the steady-state line." *Journal of Geotechnical and Geoenvironmental Engineering*, ASCE, 123(3): 281 - 288.
- Sadrekarami, A. (2009). "Development of a new ring shear apparatus for investigating the critical state of sands." Ph.D. thesis, University of Illinois, Urbana-Champaign, Urbana, Illinois.
- Sasitharan, S. (1994). "Collapse behavior of very loose sand." PhD, University of Alberta, Edmonton, Alberta.
- Sasitharan, S., Robertson, P. K., Segoo, D. C., and Morgenstern, N. R. (1993). "Collapse behavior of sand." *Canadian Geotechnical Journal*, 30(4): 569 - 577.
- Sasitharan, S., Robertson, P. K., Segoo, D. C., and Morgenstern, N. R. (1994). "State-boundary surface for very loose sand and its practical implications." *Canadian Geotechnical Journal*, 31(3): 321-334.
- Sassa, K. (1998). "Mechanisms of Landslide Triggered Debris Flows." *Proceedings of the IUFRO Division 8 Conference Environmental Forest Science*, pp. 499 - 518.
- Shahsavari, M. (2012). "Effect of initial shear stress direction and stress history on the undrained behaviour of sands under triaxial loading." MSc, Carleton University, Ottawa.
- Sivathayalan, S., and Vaid, Y. P. (2002). "Influence of generalized initial state and principal stress rotation on the undrained response of sands." *Canadian Geotechnical Journal*, 39(1): 63-76.
- Skirrow, R. K. (1996). "The effects of fines content on the monotonic triaxial testing of cohesionless soils for evaluation of in-situ state." MSc, University of Alberta, Edmonton.
- Sladen, J. A., and Handford, G. (1987). "A potential systematic error in laboratory testing of very loose sands." *Canadian Geotechnical Journal*, 24(3): 462 - 466.
- Stiber, N. A. (1992). "Undrained steady state strength of fine sands under axisymmetric conditions." MSc, Northwestern University, Evanston.
- Take, W. A., Beddoe, R. A., Davoodi-Bilesavar, R., and Phillips, R. (2013). "Effect of antecedent groundwater conditions on the triggering of static liquefaction landslides." *Landslides*, 12(3): 469 - 479.
- Takehita, S., Takeishi, M., and Tamada, K. (1995). "Static liquefaction of sands and its liquefaction index." Proc., 1st International Conference on Earthquake Geotechnical Engineering, A.A. Balkema, Rotterdam, The Netherlands, pp. 177 - 182.
- Tsomokos, A., and Georgiannou, V. N. (2010). "Effect of grain shape and angularity on the undrained response of fine sands." *Canadian Geotechnical Journal*, 47(5): 539 - 551.
- Uthayakumar, M., and Vaid, Y. P. (1998). "Static liquefaction of sands under multiaxial loading." *Canadian Geotechnical Journal*, 35(2): 273 - 283.
- Vaid, Y. P., and Chern, J. C. (1983). "Effect of static shear on resistance to liquefaction." *Soils and Foundations*, 23(1): 47 - 60.
- Vaid, Y. P., Stedman, J. D., and Sivathayalan, S. (2001). "Confining stress and static shear effects in cyclic liquefaction." *Canadian Geotechnical Journal*, 38(3): 580-591.
- Vaid, Y. P., and Thomas, J. (1995). "Liquefaction and postliquefaction behavior of sand." *Journal of Geotechnical Engineering*, ASCE, 121(2): 163 - 173.
- Verdugo, R. (1992). "Characterization of sandy soil behavior under large deformation." PhD, University of Tokyo, Tokyo, Japan.
- Wanatowski, D., and Chu, J. (2007). "K₀ of sand measured by a plane-strain apparatus." *Canadian Geotechnical Journal*, 44(8): 1006-1012.
- Wang, G. (1999). "An experimental study on the mechanism of fluidized landslide." PhD, Kyoto University, Kyoto.
- Wang, G., and Sassa, K. (2003). "Pore-pressure generation and movement of rainfall-induced landslides: effects of grain size and fine-particle content." *Engineering Geology*, 69(1-2): 109 - 125.
- Wang, J. (2005). "The Stress-Strain and Strength Characteristics of Portaway Sand." PhD Dissertation, The University of Nottingham, Nottingham, UK.
- Wride, C. E., and Robertson, P. K. (1997a). "Phase I and III data review report (Mildred Lake and J-pit sites, Syncrude Canada Ltd.)." *CANLEX Technical Report*, University of Alberta, Edmonton.
- Wride, C. E., and Robertson, P. K. (1997b). "Phase II data review report (Massey and Kidd sites Fraser River delta)." *CANLEX Technical Report*, University of Alberta, Edmonton.
- Yoshimine, M. (1996). "Undrained flow deformation of saturated sand under monotonic loading conditions." PhD, University of Tokyo, Tokyo.
- Yoshimine, M., and Ishihara, K. (1998). "Flow potential of sand during liquefaction." *Soils and Foundations*, 38(3): 187 - 196.
- Yoshimine, M., Ishihara, K., and Vargas, W. (1998). "Effects of principal stress direction and intermediate principal stress on undrained shear behavior of sand." *Soils and Foundations*, 38(3): 179-188.
- Yoshimine, M., Robertson, P., and Wride, C. E. (2001). "Undrained shear strength of clean sands to trigger flow liquefaction: Reply." *Canadian Geotechnical Journal*, 38(3): 654-657.
- Yoshimine, M., Robertson, P. K., and Wride, C. E. (1999). "Undrained shear strength of clean sands to trigger flow liquefaction." *Canadian Geotechnical Journal*, 36(5): 891-906.
- Zhang, H. (1997). "Steady state behaviour of sands and limitations of the triaxial test." PhD, University of Ottawa, Ottawa.
- Zhang, H. M., and Garga, V. K. (1997). "Quasi-steady state: a real behaviour?" *Canadian Geotechnical Journal*, 34(5): 749-761.